

Diagnosis for Sucker Rod Pumps Using Bayesian Networks and Dynamometer Card

Boyuan Zheng, Xianwen Gao

College of Information Science and Engineering
Northeastern University
Shengyang, China
zhengboyuanneu@163.com
gaoxianwen@mail.neu.edu.cn

Rong Pan

School of Computing, Informatics, and Decision Systems
Engineering
Arizona State University
Tempe, USA
Rong.Pan@asu.edu

Abstract—The automatic diagnosis for sucker rod pump (SRP) is an essential measurement to ensure the oil fields' interests in the oil recovery. As the important information resource on monitoring and diagnosis, the dynamometer card (DC) plays an irreplaceable role in oil engineering. In the application, how to use DC to fulfill the diagnosis is always the key to this problem. Thus, a novel method based on load analysis and Bayesian network is proposed in this paper. At first off, DC's coordinate is transformed to cater to the load analysis, which provides an instinctive way for analyzing. After that, five statistical features and Shannon entropy are extracted from the DC, which are employed as the input of the Bayesian network (BN) presented in the particular framework. At last, a set of field dynamometer card is employed as the experimental data and the experimental results demonstrate the feasibility and superiority of the proposed method for diagnosing the working states of SRPs.

Keywords—*Bayesian network classifier; Sucker rod pump; Dynamometer card; Diagnosis*

I. INTRODUCTION

Suck rod pumps are the most widely used artificial lift technique in the oilfields, which have applied to about 80% oil wells in the world [1]. In the process of pumping oil up to the surface, this equipment's down-hole part always in the underground of thousands of meters deep. The harsh working circumstance in the underground often results in some faulty working states that may influence the oil yield and management cost. However, the working state in the down-hole is difficult to monitor directly by sensors. Hence, it is meaningful to take effective measures to deal with this issue [2].

Dynamometer card [3, 4] is a closed curve composed by the movement vs load, which plays an essential role in oil wells' monitoring. Trained engineers could judge the down-hole working state according to the shape of this curve. Nevertheless, this manual method is restricted by the engineers' subjective knowledge and not able to perform the real-time diagnosis, which could not fit the further interest of

oil field.

For the sake of implementing timely diagnosis, a great amount of researchers concentrated on this open issue and published many effective methods in their papers. Their main contributions can be concluded in two aspects. Regarding the feature extraction, Zhong [5] mapped the dynamometer card into a gray space and carried out the grey scale analysis. He et al. [6] utilized the spectrum analysis to compute the properties of DCs under different working states. Li et al. [7] adopted Freeman Chain Code to analyze the DCs' features under various working states. Gao et al. [8] implemented the feature extraction for DCs based on the curve moments. On the other hand, with the rapid development of statistical models such as Neural Network [9], Support Vector Machine [10], Extreme Learning Machine [11], are employed to solve the diagnosis problem for SRP. However, these data-driven models overly rely on the quality and quantity of samples and neglect the mechanism of DCs' forming process. The Bayesian Network, a kind of probabilistic graphical models, has been a widely used classifier in the different contexts due to clear structure and outstanding performance [12].

Depending on the foregoing discussion, this paper presents a novel approach to cope with the diagnosis of the SRP. The contributions of the proposed method can be summarized as follows. At first off, DC's abscissa is transformed into a stroke to support the subsequent analysis. After that, five statistic and Shannon entropy are proposed to describe the DCs form different perspectives. After that, a diagnosis model is built under a particular type of BN named Multiple Gaussian Network (MGN). At last, a case study on an oil field data set is carried out to demonstrate superiority and the capability of the proposed method.

The layout of this paper is as follows. Section 2 presents several features of DC based on the mechanism SRP. Section 3 employ the BN as the classifier to fulfill the diagnosis in a specific framework. Several experiments verified the propose method based on field data in Section 4. Finally, Section 5 gives the conclusion of this paper.

II. FEATURE EXTRACTION FROM DYNAMOMETER CARD

Considering the data characteristics of DCs, in this section, we take the statistical features and Shannon energy entropy to carry out feature extraction.

A. Sucker rod pump and dynamometer card

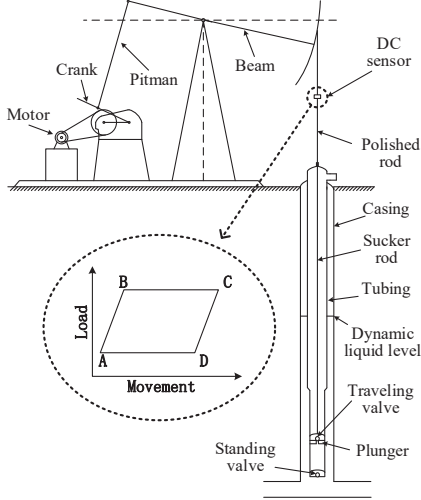


Figure 1. Sucker rod pump system DC

As shown in Figure 1, the SRP system and the theoretical DC are presented in this picture. This system has two main components that are the surface and down-hole. On the surface, the linkages transfer the motor's rotational motion to the up-and-down movement on the polished rod. In the underground, the essential component is the pump immersed in the dynamic liquid level, which is connected by a long metal rod, called sucker rod, from the surface. Notably, the DC sensor on the polished rod is used to collect DC by detecting the movement and load in one stroke.

In the normal working state, the shape of DC approximates to a parallelogram that is shown in the left-down in Figure 1. The parallelogram locals in a two-dimension coordinate that the ordinate is load and the abscissa is the movement. For convenience, the four corners are marked A, B, C, and D. According to the mechanism of the pump, the parallelogram can be divided into four parts (A-B, B-C, C-D, and D-A) that reflect the working process at the different stages in one cycle. When the SRP works at faulty working state, the shape of DC will generate apparent changes at corresponding parts.

B. Features extraction

Feature extraction has a decisive influence on the modeling and testing in the diagnosis. Thus, a proper feature extraction method is the precondition for following diagnosis. According to the above discussed, DC can be treated as a vibration signal that period is the time consumption of one stroke. Especially, when replacing the movement as the stroke on the abscissa, as shown in the Figure2, the load curve is demonstrated in a more instinctive way, which is no longer a closed curve and instead be a continuous signal going with time.

In the applications of vibration signals analysis, the statistical features and the Shannon entropy are commonly

used methods for signal analysis. The statistical features focus on calculating the shape and distribution, and the Shannon entropy is mainly to measure the uncertainty and randomness of a signal. Therefore, this research takes these two methods to analyze DCs.

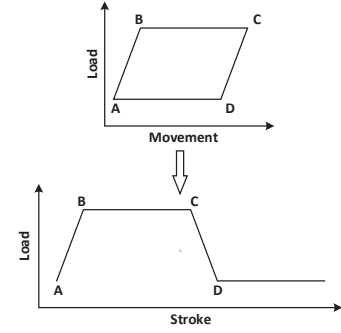


Figure 2. Coordinate transformation of DC

1) *Statistical features:* Considering the properties of the signal in Figure 2, here are several statistical features formulas that were appointed in the follows.

The first statistical feature is the ratio between the maximum load and the minimum load in a stroke.

$$\eta = \frac{\max(x) - \min(x)}{\max(x)} \quad (1)$$

where $\max(\cdot)$ is the maximal load and the $\min(\cdot)$ is the minimal load.

The second statistical feature is the Root Mean Square that is frequently used to imply the degree of fluctuation.

$$RMS = \sqrt{\frac{\sum_{i=1}^n (x_i - \mu)^2}{n}} \quad (2)$$

The third statistical feature is the skewness that can calculate the horizontal changes in the load signal.

$$Skewness = \sqrt{\frac{\sum_{i=1}^n (x_i - \mu)^2}{\sigma^2}} \quad (3)$$

where σ is the standard deviation and the μ is the load average.

The Kurtosis is employed as the fourth statistical feature, which can identify the vertical changes in the load signal.

$$Kurtosis = \sqrt{\frac{\sum_{i=1}^n (x_i - \bar{x})^4}{\sigma^4}} \quad (4)$$

The shape factor is the fifth statistical feature:

$$\text{Shape factor} = \frac{\sqrt{\sum_{i=1}^n x_i}}{\sum_{i=1}^n x_i} \quad (5)$$

2) *Shannon energy entropy*: Shannon entropy is a useful way to measure the uncertain and random part in data, which is widely used in the signal analysis. In general speaking, this kind of information entropy always give small value while the signal is well regulated, on the contrary, the values will go up in the faulty working states according to the different detective degrees. Therefore, Shannon entropy can imply the quantity and distribution of the information in the load signal so well that it can be employed to characterize the faulty working states. When some faults occur, the shape of the load curve is no longer as it showed is in the normal shown in Figure 2. Given a load signal $x(t)$ in one stroke, the Shannon energy entropy can be calculated by the follows:

$$\text{EDC} = -\sum_{t=1}^T x(t) \ln x(t) \quad (6)$$

III. DYNAMIC BAYESIAN NETWORK FOR SRP DIAGNOSIS

A. Preliminaries

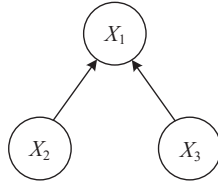


Figure 3. A BN example with three nodes

A Bayesian Network (BN) is one kind of the probabilistic graphical models that defined as a causal network, which is instinctive to show the knowledge in the graphical form [18]. A directed acyclic graph includes many nodes representing random variables and arcs indicating the probabilistic dependencies between connected nodes. For general speaking, BN is a graphical model that illustrates the probabilistic causal relationship between random variables and the direction of information flow [19]. In a BN, the parent node is designed to provide the arcs to its following child nodes. The node without any parent node is called the root node and the node does not have any child node is named leaf node. Otherwise, an arc from a child node can never come back to its parent nodes. There is a BN example shown in Figure 3. In this figure, X_2 and X_3 are the parent nodes of X_1 and the root nodes of the entire network. On another hand, the X_1 is the child node of X_2 and X_3 and a leaf node of this network [20].

As the working foundational part, the joint probability distribution of the network can be ensured through the chain rule according to the topology of BN, which can be implied as:

$$P(X_1, X_2, \dots, X_n) = \prod_{i=1}^n P(X_i / Pa(X_i)) \quad (7)$$

where $Pa(X_i)$ is the parent set of any node X_i .

B. SRP diagnosis based on conditional Gaussian network

In this paper, six working states are considered, which means that the data set consist of six classes. Thus, we describe the observation set as follows:

$$O^{(N)} = \{O^1, O^2, \dots, O^N\} \quad (8)$$

$$O^i = \{O_1^i, O_2^i, \dots, O_T^i\} \quad (9)$$

where O^i is the observation sequence of i th working state and O_j^i is a feature vector extracted from the j th motor power curve at the i th working state through the proposed method in Section II.

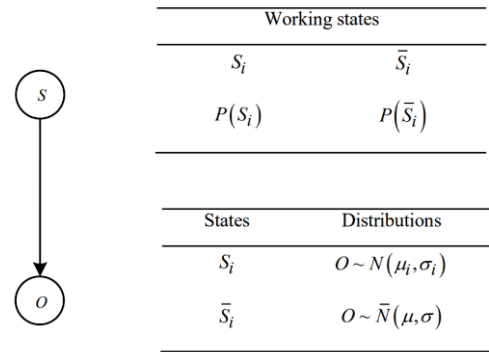


Figure 4. CGN for SRP diagnosis

As the operation of SRP is a dynamic process with continuous observations, it is not justified if we used conventional BN to capture the dynamic properties. Therefore, in this paper, a particular type of BN named Conditional Gaussian Network (CGN) is used to realize the probabilistic inference of continuous variable.

There are two types of nodes in CGN, respectively discrete nodes and Gaussian nodes. In this network, discrete nodes are not allowed to have continuous parents. On the contrary, the Gaussian nodes could have both kinds of parent nodes [21]. If a Gaussian node Y only has one discrete parent node X , $X = \{X_1, \dots, X_k\}$, the conditional distribution of Y given one state of X can be described as below:

$$P(Y | X = X_k) = N(\mu_k, \sigma_k) \quad (10)$$

Figure 4 gives an example regarding CGN-based model for dealing with the diagnosis problem in this paper.

As six working states are considered in this paper, in this paper we construct a Multiple BNs (MBNs) to fit the observations from different wells. A set of models that are defined as follows:

$$\Theta^{(N)} = \{\Theta_1, \Theta_2, \dots, \Theta_N\} \quad (11)$$

TABLE I. AVERAGE FEATURE AT SIX WORKING STATES

Working states	Features					
	η	<i>RMS</i>	<i>Skewness</i>	<i>Kurtosis</i>	<i>Shape factor</i>	<i>EDC</i>
Normal	0.5268	0.3812	-0.0023	1.1782	0.0077	2.4514
Gas affected	0.3966	0.2789	-0.0793	1.4486	0.0150	2.9098
Insufficient Liquid Supply	0.4394	0.2540	-0.4846	1.9315	0.0103	2.8459
Standing valve leakage	0.5766	0.3917	-0.2907	1.3161	0.0100	2.5815
Parting rod	0.1568	0.4061	-0.0030	1.1916	0.0122	2.5033
Gas locked	0.3085	0.3380	-0.8615	2.1864	0.0060	2.6376

where $\Theta^{(N)}$ is the model parameter set and Θ_i is the model of the i th working state. This model set contains N binary models corresponding to the N considered working states. Regarding the i th model, the modeling process is as follows:

Step 1: Configure the structure based on process dynamics.

Step 2: Set the prior probability distribution.

Step 3: Repeat inputting the samples in O^i to Θ_i one by one and update the belief at each sample.

Repeat this method all the models in this training process until all the models in (11) are obtained.

As for giving a label for new-coming samples, using the trained models, the performing process is as follows. Assume O_{T+1} is a new-coming sample at time $T+1$. We can input this sample to the $\Theta^{(N)}$ and compare the probabilities obtained from these six models, this process can be implied using (12).

$$S_P = \arg \max_{s_i \in S} P(O_{T+1} | s_i) \quad (12)$$

IV. EXPERIMENTAL RESULTS

In this section, the experimental results are provided to demonstrate the implementing process and the capability of the proposed method for working state diagnosis.

A. Experimental data and pre-processing

To supporting the research of this experiment, a set of dynamometer cards are collected from an oil field. In this set, six working states are included, respectively normal, gas affected, insufficient liquid supply, gas lock, standing valve leakage, and parting rod. These six are the most commonly happened working states in the SRP's running process. There are 120 dynamometer cards in this set. 20 samples are at normal, 20 samples are at gas affected, 20 samples are at insufficient liquid supply, 20 samples are at gas lock, 20 samples are at the standing valve leakage, 20 samples are at parting rod.

Before carrying out the experiment, we organize this set in parts, especially for training and testing. As for each working state, last five samples are employed as the testing samples and the reminding samples are utilized to build models.

Furthermore, as the DCs collected from wells always have different range on the working coefficients on load and movement. In order to eliminate influences caused by the differences between wells. The normalization is supposed to be applied. Assume the every DC composes of discrete points $\{(x_i, y_i)\}$:

$$\tilde{x} = \frac{x_i - x_{\min}}{x_{\max} - x_{\min}} \quad (13)$$

$$\tilde{y} = \frac{y_i - y_{\min}}{y_{\max} - y_{\min}} \quad (14)$$

where x_i and y_i are the movement and the load.

Figure 6 gives an example on DC coordinate transformation at six working states, which implies the load change with time in an instinctive way. These six curves show the differences in the globe and local parts. To quantify the characters of each curve, the proposed features are used to describe the characteristics of these curves in the following experiment.

B. Feature extraction

The study that showed in Table I gives the average value of the proposed features based on the experimental data set. In this table, every working state embodies the unique characteristics on particular features. Conspicuously, the normal working state has a larger value for η , *skewness*, *EDC* and a smaller value for *kurtosis*, *shape factor*. Diversely, the six features imply different variations under other working states. For example, the insufficient liquid supply shows the higher kurtosis and EDC, the gas effected gives the highest RDC, relatively low RMS. Especially for the gas locked and the parting rod, they reveal more apparent characteristic on η ,

TABLE II. CONFUSION MATRIX FOR THE DIAGNOSIS RESULTS OF THE PROPOSED METHOD

Diagnosed pattern	Happening pattern					
	<i>Normal</i>	<i>Insufficient Liquid Supply</i>	<i>Gas affected</i>	<i>Gas locked</i>	<i>Standing valve leakage</i>	<i>Parting rod</i>
Normal	4	0	1	0	0	0
Insufficient Liquid Supply	0	4	1	0	0	0
Gas affected	1	0	4	0	0	0
Gas locked	0	0	0	5	0	0
Standing valve leakage	1	0	0	0	4	0
Parting rod	0	0	0	0	0	5

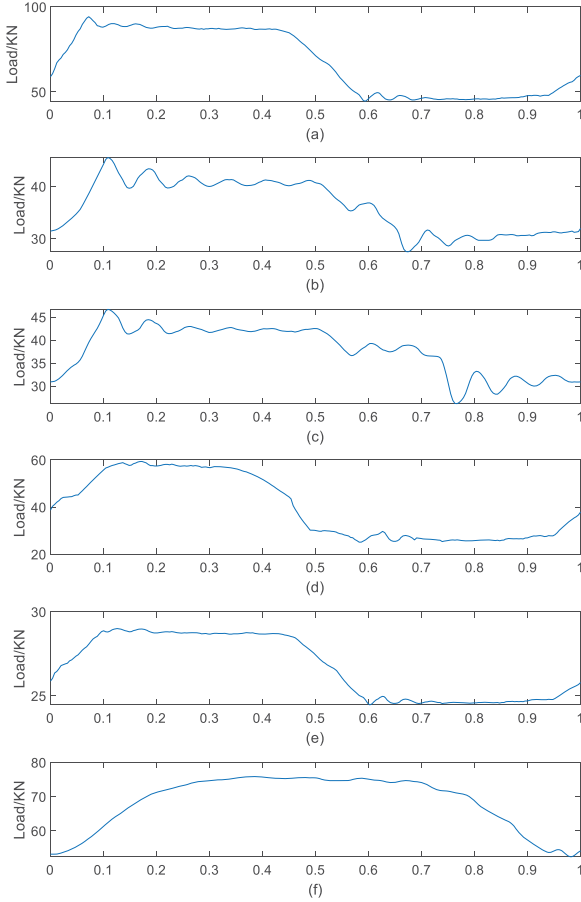


Figure 5. Coordinate transformation under various working states. (a) Normal. (b) Gas affected. (c) Insufficient liquid supply. (d) Standing valve leakage. (e) Parting rod. (f) Gas locked.

RMS, shape factor, and *EDC*. These obvious differences are mainly caused by two reasons. One is the result based on the statistical analysis. As for the other reason is the Shannon describes uncertain and random degree at every working state.

TABLE III. COMPARISON RESEARCH WITH OTHER METHODS

Features	Models		
	ELM	SVM	BNs
FFT	63.3%	76.6%	83.3%
Curve moment	63.3%	73.3%	80%
Proposed features	70.0%	80%	86.6%

C. Proposed method for SRP diagnosis

We employ the proposed BNs, introduced in Section 3, as the classifiers to perform the diagnosis. Table II provides a confusion matrix to demonstrate the diagnosis results. As shown in this table, five misclassifications occur from a total of 30 samples in the testing set. Among the misclassifications, two normal are wrongly classified as the gas affected and standing valve leakage respectively. One insufficient liquid supply is recognized as the gas affected. One gas affected and one standing valve leakage are wrongly diagnosed as normal.

In order to further testify the proposed method, a comparison research is carried out. As shown in Table III, two modeling method, ELM and SVM, and feature extraction methods, FFT and curve moment, are employed in this study. In this table, the ELM gives the lowest accuracy based on FFT and curve moment, only 63.3%. The SVM shows higher accuracy comparing with the ELM, the BNs based on the proposed features gives the highest accuracy 86.6%.

D. Discussion for the diagnosis results

Among the considered six working states, the gas lock and the parting rod belong to primary faults that are required to terminate the operation of the SRP once these two working states are detected, in case of causing the damages on the mechanical and electric components. In addition, the other three detective working states are the secondary faults, which need to be monitored closely but unnecessary to shut down the

wells. According to the diagnosis, it is easy to find that there is no misclassification at the two primary faults, namely gas lock and parting rod. On the other hand, sometimes, the boundaries between working states are so ambiguous that even if experienced engineers as well give a clear diagnosis. Hence, the diagnosis results of this paper are reasonable and acceptable in the application.

V. CONCLUSION

For implementing the automatic diagnosis for SRP, a new dynamometer card-based method is proposed in this paper. First off, the coordinates of dynamometer cards are transformed into the stroke, which offers an instinctive way to support the following analysis. After that, six novel features are proposed according to the statistical variables and Shannon entropy. A set of Bayesian networks in a particularly designed framework is used as the classifier to carry out the diagnosis. At last, a dynamometer card set collected from the oil field is used to support this research and the experimental results demonstrate the proposed method's feasibility in the application.

REFERENCES

- [1] Bogdan M. Wilamowski and Okyay Kaynak, "Oil well diagnosis by sensing terminal characteristics of the induction motor," *IEEE Transactions on Industrial Electronics*, vol. 47, pp. 1100–1107, July 2000.
- [2] R. Luo, C. Lu, and X. Jing, "Research on fault diagnosis of sucker rod pumps based on analysis of indicator diagram," *Computer measurement control (in Chinese)*, vol. 24, pp. 46–49, Jan. 2016.
- [3] K Li, X. Gao, and H. Zhou, "Diagnosis for down-hole conditions of sucker rod pumping system based on the FBH-SC method. *Petroleum Science*," vol. 12, pp. 135–147, Jan. 2015.
- [4] B. Zheng and X. Gao, "Sucker rod pumping diagnosis using valve working position and parameter optimal continuous hidden Markov model," *Journal of Process Control*, vol. 59, pp. 1–12, Oct. 2017.
- [5] G. Zhong and M. Zou, "Exploring Failure Characteristics of Indicator Diagram of Reciprocating Pump Based on Gray Matrix," *Mechanical Science and Technology for Aerospace Engineering*, vol. 35, pp. 279–284, Sep. 2016.
- [6] Y. He, X. Wu and G. Han, "Frequency spectrum analysis method for recognition of dynamometer card," *ACTA PETROLEUM SINICA (in Chinese)* vol. 29, pp. 619–624, July 2008.
- [7] K. Li, X. Gao, W. Yang, et al., "Multiple fault diagnosis of down-hole conditions of sucker-rod pumping wells based on Freeman chain code and DCA," *Petroleum Science*, vol.10, pp. 347–360, Sep. 2013.
- [8] G. Gao, Y. Peng, G. Yu, et al., "Quantitative analysis of dynamometer cards for sucker rod pumping wells," *Acta Petrolei Sinica*. vol. 14, pp. 141–150, Dec. 1993.
- [9] P. Xu, S. Xu, and H. Yin, "Application of self-organizing competitive neural network in fault diagnosis of sucker rod pumping system," *Journal of Petroleum Science and Engineering*, vol. 58, pp. 43–48, Nov. 2006.
- [10] K Li, X. Gao, Z. Tian, et al., "Using the curve moment and the PSO-SVM method to diagnose downhole conditions of a sucker rod pumping unit," *Petroleum Science*, vol.10, pp. 73–80, Feb. 2013.
- [11] K. Li, Y. Han, and T. Wang, "A novel prediction method for down-hole working conditions of the beam pumping unit based on 8-directions chain codes and online sequential extreme learning machine," *Journal of Petroleum Science and Engineering*, vol. 160, pp. 285–301, Oct. 2017.
- [12] J. Bermana, D. Francoza, S. Dufourb, S. Buczinskia, "Bayesian estimation of sensitivity and specificity of systematic thoracic ultrasound exam for diagnosis of bovine respiratory disease in pre-weaned calves," *Preventive Veterinary Medicine*, vol. 162, pp. 38–45, Oct. 2018.
- [13] B. Cai, H. Liu, and M. Xie, "A real-time fault diagnosis methodology of complex systems using object-oriented Bayesian networks," *Mechanical Systems and Signal Processing*, vol. 80, pp. 31–44, April 2016.
- [14] S. Buczinski, G. Fecteau, and J. Dubuc, "Validation of a clinical scoring system for bovine respiratory disease complex diagnosis in preweaned dairy calves using a Bayesian framework," *Preventive Veterinary Medicine*, Vol. 156, pp. 102–112, May 2018.
- [15] F. Qi and Biao Huang, "Bayesian methods for control loop diagnosis in the presence of temporal dependent evidences," *Automatica*, vol. 47, pp. 1349–1356, Mar. 2011.
- [16] S. He, Z. Wang, Z. Wang, X. Gu, Z. Yan, "Fault detection and diagnosis of chiller using Bayesian network classifier with probabilistic boundary," *Applied Thermal Engineering*, vol.107, pp. 37–47, Jun. 2016.
- [17] G. Wua, J. Tong, L. Zhang, Y. Zhao, Z. Duan, "Framework for fault diagnosis with multi-source sensor nodes in nuclear power plants based on a Bayesian network," *Annals of Nuclear Energy*, vol. 122, pp. 297–308, Sep. 2018.
- [18] F. Nir, and D. Koller, "Being Bayesian about Network Structure. A Bayesian Approach to Structure Discovery in Bayesian Networks," *Machine learning*, vol. 50, pp. 95–125, Sep. 2001.
- [19] S. Mahadevan, R. Zhang, and N. Smith, "Bayesian Networks for System Reliability Reassessment," *Structural Safety*, vol. 23, pp. 231–251, Sep. 2001.
- [20] D. Lee and R. Pan, "Predictive maintenance of complex system with multi-level reliability structure," *International Journal of Production Research*, DOI: 10.1080/00207543.2017.1299947, May 2017.
- [21] S.L. Lauritzen and F. Jensen, "Stable local computation with conditional Gaussian distributions," *Statistics Comput.*, vol. 11, pp. 191–203, Sep. 1993.